Deep inelastic scattering from $A=3$ nuclei and the neutron structure function

I. R. Afnan,[1] F. Bissey,[2] J. Gomez,[3] A. T. Katramatou,[4] S. Liuti,[5] W. Melnitchouk,[3] G. G. Petratos,[4] and A. W. Thomas[6]
[1]*School of Physical Sciences, Flinders University of South Australia, Bedford Park 5042, Australia*
[2]*Université de Liège, Département de Physique, Institut de Physique B.5, Sart Tilman, B-4000 Liege 1, Belgium*
[3]*Jefferson Lab, 12000 Jefferson Avenue, Newport News, Virginia 23606, USA*
[4]*Kent State University, Kent, Ohio 44242, USA*
[5]*Department of Physics, University of Virginia, Charlottesville, Virginia 22904, USA and INFN, Sezione di Roma Tre, Via della Vasca Navale, 00184 Roma, Italy*
[6]*Special Research Centre for the Subatomic Structure of Matter, and Department of Physics and Mathematical Physics, University of Adelaide, Adelaide 5005, Australia*
(Received 2 April 2003; published 4 September 2003)

We present a comprehensive analysis of deep inelastic scattering from ^{3}He and ^{3}H, focusing in particular on the extraction of the free neutron structure function F_2^n. Nuclear corrections are shown to cancel to within 1–2% for the isospin-weighted ratio of ^{3}He to ^{3}H structure functions, which leads to more than an order of magnitude improvement in the current uncertainty in the neutron to proton ratio F_2^n/F_2^p at large x. Theoretical uncertainties originating from the nuclear wave function, including possible non-nucleonic components, are evaluated. Measurements of the ^{3}He and ^{3}H structure functions will, in addition, determine the magnitude of the EMC effect in all $A \leqslant 3$ nuclei.

DOI: 10.1103/PhysRevC.68.035201 PACS number(s): 13.60.Hb, 21.45.+v, 14.20.Dh

I. INTRODUCTION

It is a somewhat anomalous situation whereby the nuclear effects in deep inelastic scattering (DIS) from few-nucleon systems, for which the theoretical descriptions are most easily tractable, namely the deuteron, helium-3, and tritium, are the least well known experimentally. For example, the nuclear EMC effect has been extensively studied for $4<A \lesssim 200$ [1]; but 20 years after the original EMC observation [2] of nucleon structure function modification in medium, it is still not known for $A=2$ or 3 systems.

The lack of knowledge of the EMC effect in $A<4$ nuclei has been a major obstacle to a complete description of the nucleon structure functions themselves. The distribution of valence u and d quarks in the proton can be determined from any two observables containing linear combinations of u and d quarks, which are usually taken to be the proton and neutron structure functions F_2^p and F_2^n. While the proton structure function is quite well constrained for light-cone momentum fractions $x=Q^2/2M\nu \lesssim 0.8$, the neutron F_2^n is usually extracted from data on deuterium, however, beyond $x\sim 0.5$ the large nuclear corrections can result in uncertainties of up to $\sim 50\%$ in F_2^n/F_2^p [3–7]. Here, Q^2 is minus the photon virtuality and ν its energy, while M is the nucleon mass. Inclusive proton and deuteron data, which have been almost exclusively been used to constrain the d/u ratio, are therefore unreliable for determining the neutron structure function beyond $x\sim 0.5$, and other methods must be sought.

Several alternatives for obtaining an independent linear combination of u and d quark distributions have been discussed recently, which could minimize or avoid the problem of nuclear corrections. These include flavor tagging in semi-inclusive scattering from hydrogen, in which $\pi^{\pm}$ production at large z selects u and d quarks, respectively [7], and parity-violating $\vec{e}p$ scattering, for which the left-right polarization asymmetry arising from the γ^*-Z interference is, at leading order, proportional to d/u [8]. Other proposals have utilized the weak charged current to couple preferentially either u or d flavors, for example asymmetries in W-boson production in pp and $p\bar{p}$ collisions [9] at Fermilab or RHIC, or charged current e^+p deep inelastic scattering at HERA [10]. One of the more promising techniques appears to be the semi-inclusive DIS from a deuterium target, with coincidence detection of a low momentum spectator proton in the target fragmentation region, which maximizes the likelihood of scattering from a nearly on-shell neutron [11,12].

In this paper we focus on a novel idea which would neither be subject to the low rates associated with weak current reactions nor rely on the validity of factorization of target and current hadrons in the final state in semi-inclusive scattering. It involves maximally exploiting the mirror symmetry of $A=3$ nuclei to extract the F_2^n/F_2^p ratio from the ratio of ^{3}He/^{3}H F_2 structure functions [13]. Differences in the relative size of nuclear effects in ^{3}He and ^{3}H are quite small—essentially on the scale of charge-symmetry breaking in nuclei—even though the absolute size of the EMC effect in an $A=3$ nucleus can be relatively large. Preliminary results for the expected errors in the extraction have been presented in Ref. [14]. (See also Ref. [15].) Here, we discuss in detail the possible theoretical uncertainties associated with nuclear effects in three-body nuclei and experimental considerations relevant for a clean measurement of the ^{3}He/^{3}H structure function ratio. Some of the latter have been summarized in Ref. [16]. In particular, we consider effects of different nuclear wave functions, charge-symmetry breaking, finite-Q^2 corrections, as well as non-nucleonic degrees of freedom, such as six-quark clusters, and explicit nucleon off-shell effects.

In Sec. II, we motivate the need for new measurements of the free-neutron structure function in the hitherto unexplored kinematic region at large x, and outline the extraction of F_2^n from the $F_2^{^3\mathrm{He}}$ and $F_2^{^3\mathrm{H}}$ structure functions. A detailed discussion on the theoretical framework and the nuclear spectral functions is presented in Sec. III. As well as allowing for a relatively clean extraction of the F_2^n/F_2^p ratio, deep inelastic scattering from ^{3}He/^{3}H can also provide the first indications of the absolute size of the EMC effect in $A=3$ nuclei. With the exception of the recent HERMES data [17] at lower x and Q^2 on the ratio of ^{3}He to p and d cross sections, all existing data on the nuclear EMC effect are for $A \geqslant 4$. Predictions for the EMC ratios in ^{3}He and ^{3}H based on the conventional nuclear descriptions are discussed in Sec. III.

The sensitivity of the extracted F_2^n to nuclear effects is dealt with in detail in Sec. IV, where in addition to conventional nuclear models of the $A=3$ system in terms of well-known three-body wave functions, we examine more speculative models, including those involving explicit non-nucleon degrees of freedom, in order to assess the possible model dependence of the extraction. We find that for all models which are known to be consistent with standard nuclear phenomenology, the nuclear effects in the ratio of the EMC effects in ^{3}He and ^{3}H cancel to within 1–2 % for $x \lesssim 0.8$. In Sec. V, we calculate the expected rates at which the ^{3}He and ^{3}H cross sections can be determined experimentally at future facilities, such as Jefferson Lab with 12 GeV electron energy. Finally, we summarize our findings in Sec. VI.

II. NEUTRON STRUCTURE FUNCTION AND THE $A=3$ SYSTEM

In this section, we outline the theoretical motivation for determining precisely the neutron structure function at large x, and describe in detail the method proposed to extract F_2^n from deep inelastic ^{3}He and ^{3}H structure functions.

A. Neutron structure and spin-flavor symmetry breaking

An accurate determination of the neutron structure function F_2^n is essential for pinning down the momentum dependence of both the u and d quarks in the nucleon. While the u quark distribution in the proton is relatively well determined by the proton F_2 data, the d/u ratio at large x is, at leading order, usually extracted from a ratio of the neutron to proton structure functions:

$$\frac{F_2^n}{F_2^p} = \frac{1+4d/u}{4+d/u}. \tag{1}$$

According to SU(6) symmetry one would expect that $u=2d$ for all x, so that $F_2^n/F_2^p = 2/3$, although the data have for a long time been known to deviate strongly from this naive expectation beyond $x \sim 0.4$. A number of different nonperturbative mechanisms have been suggested [18–25] which break SU(6) symmetry, and most have been able to fit the data in the region of x where n/p can be reliably extracted.

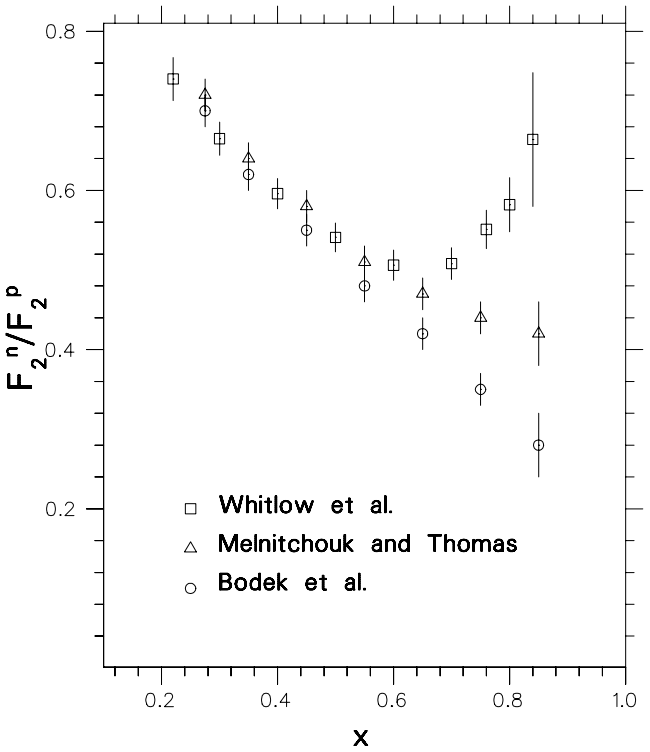

FIG. 1. Neutron to proton ratio, extracted from inclusive proton and deuteron inelastic data, correcting for the effects of Fermi motion and nuclear binding (Melnitchouk and Thomas [6]), Fermi motion only (Bodek *et al.* [27]), and using the density extrapolation model (Whitlow *et al.* [3]).

On the other hand, the $x \to 1$ behavior of F_2^n/F_2^p predicted by the various models depends rather strongly on the assumed dynamics responsible for the symmetry breaking. In particular, whether the suppression of the d quark at large x is due to suppression of helicity antialigned quarks in the proton or nonperturbative interactions which raise the energy of the scalar-isoscalar diquark components of the proton wave function, the $x \to 1$ limit of F_2^n/F_2^p can vary from 1/4 [18,19] up to 3/7 [23]. Theoretical uncertainties in the currently extracted F_2^n at large x are comparable to the differences between the $x \to 1$ behaviors. In particular, whether one corrects for Fermi motion and binding in the deuteron [6], or Fermi motion alone [26,27], the extracted F_2^n can appear to approach either of the predicted limits, as shown in Fig. 1. (This is reminiscent of the large deuteron wave function model dependence of the extracted neutron electric form factor [28].)

Apart from testing nonperturbative QCD dynamics, a very practical reason for determining large-x distributions is the need to precisely constrain the input distributions for calculations of cross sections at high energy colliders. Uncertainties in parton distributions at large x and modest Q^2 translate via perturbative QCD evolution into uncertainties at high Q^2 at lower x. This was demonstrated recently by the so-called HERA anomaly [29], in which the apparent excess of events at $x \sim 0.6$ and $Q^2 \sim 30\,000$ GeV^2, which triggered speculation about evidence of leptoquarks, could be largely explained by a small modification in the input valence distributions at $x \sim 0.8$ [30–32].

It is crucial therefore that a reliable method be found for extracting the free-neutron structure function from measured cross sections. While extracting F_2^n from nuclear cross sections at large x does require knowledge of the nuclear EMC effect, it turns out that F_2^n extracted from the ratio of deep inelastic ^{3}He and ^{3}H cross sections is, within the likely experimental errors, almost completely independent of the nuclear corrections.

B. Extraction of F_2^n from $A=3$ mirror nuclei

Because the magnitude of the nuclear EMC effect increases with the binding energy (or mass number A), light nuclei are naturally best suited for playing the role of effective neutron targets. Ideally, one should consider systems which maximize the symmetry between the binding effects on the proton and neutron. By comparing the effective ''structure function'' of a bound proton with the free-proton structure function F_2^p (see Ref. [33] for a detailed discussion about the definition of bound nucleon structure functions), one can infer the nuclear correction that must be applied to obtain the free neutron F_2^n from the bound neutron structure function. Unfortunately, the lightest system—the deuteron—is isoscalar, so that the proton and neutron information cannot be separated through inclusive scattering alone.

The three-nucleon system, on the other hand, offers a unique opportunity for isolating the nuclear effects for both the bound proton and the bound neutron with totally inclusive scattering. In a charge-symmetric world the properties of a proton (neutron) bound in a ^{3}He nucleus would be identical to that of a neutron (proton) bound in ^{3}H. If, in addition, the proton and neutron distributions in ^{3}He (and in ^{3}H) were identical, the neutron structure function could be extracted with *no nuclear corrections*, regardless of the size of the EMC effect in ^{3}He or ^{3}H separately.

In practice, ^{3}He and ^{3}H are of course not perfect mirror nuclei—their binding energies for instance differ by $\sim 10\%$—and the p and n distributions are not quite identical. However, the $A=3$ system has been studied for many years, and modern realistic $A=3$ wave functions are known to a rather good accuracy. In a self-consistent framework one can use the same NN interaction to describe the two-nucleon system (NN scattering, deuteron form factors, quasielastic eD scattering, etc.) as well as to provide the basic input interaction into the three-nucleon calculation. Therefore, the wave functions can be tested against a large array of observables which put rather strong constraints on the models.

We start by defining the EMC-type ratios for the ^{3}He and ^{3}H structure functions (weighted by corresponding isospin factors):

$$R(^3\mathrm{He}) = \frac{F_2^{^3\mathrm{He}}}{2F_2^p + F_2^n}, \tag{2}$$

$$R(^3\mathrm{H}) = \frac{F_2^{^3\mathrm{H}}}{F_2^p + 2F_2^n}. \tag{3}$$

The ratio of these,

$$\mathcal{R} = \frac{R(^3\mathrm{He})}{R(^3\mathrm{H})}, \tag{4}$$

can be inverted to yield the ratio of free neutron to proton structure functions,

$$\frac{F_2^n}{F_2^p} = \frac{2\mathcal{R} - F_2^{^3\mathrm{He}}/F_2^{^3\mathrm{H}}}{2F_2^{^3\mathrm{He}}/F_2^{^3\mathrm{H}} - \mathcal{R}}. \tag{5}$$

If the neutron and proton distributions in the $A=3$ nuclei are not dramatically different, one might expect $\mathcal{R} \approx 1$. We stress that F_2^n/F_2^p extracted from Eq. (5) does not depend on the size of the EMC effect in ^{3}He or ^{3}H, but rather only on the *ratio* of EMC effects in ^{3}He and ^{3}H. In the following sections, we show that while the variation in the $A=3$ EMC effect can be up to 5% at large x, the deviation from unity of the ratio $\mathcal{R}$ is typically less than 1%, and is essentially independent of the model wave function.

III. DEEP INELASTIC SCATTERING FROM $A=3$ NUCLEI

In this section we outline the theoretical framework used to describe deep inelastic structure functions from nuclei in terms of nucleonic degrees of freedom. Corrections to this approach will be discussed in Sec. IV.

A. Impulse approximation

The standard framework within which nucleon Fermi motion and the binding effects are described in deep inelastic scattering from a nucleus at large x ($x \gtrsim 0.4$) is the nuclear impulse approximation, in which the virtual photon scatters incoherently from individual nucleons in the nucleon. Earlier calculations of the EMC effect in $A=3$ nuclei within this approach were reported in Ref. [34].

The nuclear cross section is calculated by factorizing the γ^*-nucleus interaction into γ^*-nucleon and nucleon-nucleus amplitudes. In the absence of relativistic and nucleon off-shell corrections [33,35,36,38] (which for the deuteron were shown [39] to be negligible, and which are also expected to be small for $A=3$), the nuclear structure function can then be calculated by smearing the nucleon structure function with a nucleon momentum distribution in the nucleus [40].

Corrections to the impulse approximation appear in the guise of final state interactions (interactions between the nucleon debris and recoil nucleus remnants), multiple rescattering of the virtual photon from more than one nucleon, as well as scattering from possible non-nucleonic constituents in the nucleus. The rescattering corrections are known to be important at small x, giving rise to nuclear shadowing for $x \lesssim 0.1$ [41], while meson-exchange currents (at least for the case of the deuteron) give rise to antishadowing at small x [42,43]. Although there is strong evidence for a role for virtual Δ's in *polarized* deep inelastic scattering on ^{3}He [37], there is as yet no firm evidence of a role for non-nucleonic degrees of freedom in unpolarized, nuclear deep inelastic scattering.

Within the impulse approximation, in the region $0.3 \lesssim x \lesssim 0.9$, the structure function F_2^A of a nucleus with mass number A can be written (to order p^2/M^2 in the nucleon momentum) as

$$F_2^A(x,Q^2) = \int d^4p \left(1 + \frac{p_z}{p_0}\right) S(p) \mathcal{F}(p,Q^2) F_2^N(x/y, Q^2, p^2), \tag{6}$$

where p is the momentum of the bound nucleon, $y = (p_0 + p_z)/M$ is the light-cone fraction of the nuclear momentum carried by the nucleon, and $S(p)$ is the nucleon spectral function (see Sec. III B below). The kinematic factor $\mathcal{F}$ contains finite-Q^2 corrections [44],

$$\mathcal{F} = \left(1 + \frac{4Mp_z x^2 r}{yQ^2}\right)^2 - (2p^2 - p_z^2)\frac{r^2x^2}{y^2Q^2}, \tag{7}$$

where $r = \nu/|\vec{q}| = 1/\sqrt{1 + 4M^2x^2/Q^2}$, and ν and $|\vec{q}|$ being the energy and the three-momentum transfer, respectively, so that $\mathcal{F} \to 1$ as $Q^2 \to \infty$. The function F_2^N is the structure function of the bound (off-shell) nucleon, which in general depends on the nucleon virtuality, $p^2 \neq M^2$. For nonrelativistic systems, and away from the very large-y region, the nucleon will not be very far off-shell, so that F_2^N can be well approximated by the free-nucleon structure function (although in the numerical results below, we will consider the sensitivity of our results to the p^2 dependence of F_2^N). If F_2^N is independent of p^2, one can factorize this from the rest of the integrand in Eq. (6), which enables one to write a simple convolution formula for the nuclear structure function,

$$F_2^A(x,Q^2) = \int_x^A dy \; f(y,Q^2) \; F_2^N(x/y,Q^2) \equiv f \otimes F_2^N, \tag{8}$$

where the function $f(y,Q^2)$ gives the light-cone distribution of nucleons in the nucleus, and is related to the nucleon spectral function $S(p)$ by

$$f(y,Q^2) = \int d^4p \left(1 + \frac{p_z}{p_0}\right) \delta\left(y - \frac{p_0 + p_z}{M}\right) S(p) \mathcal{F}(p,Q^2). \tag{9}$$

In the limit $Q^2 \to \infty$, the function $f(y,Q^2)$ reduces to the familiar Q^2 independent function

$$f(y) = 2\pi My \int_{E_{\min}} dE \int_{p_{\min}(y,E)}^{\infty} d|\vec{p}||\vec{p}| S(p), \tag{10}$$

where E is the separation energy, and where the lower limit on the p integration is given by [45]

$$p_{\min}(y,E) = \frac{1}{2}\left|\frac{\zeta^2 + 2M_{A-1}^* \zeta}{\zeta + M_{A-1}^*}\right|, \tag{11}$$

with $\zeta = M(1-y) - E$ and M_{A-1}^* is the mass of the (possibly excited) residual nucleus.

The derivation of the impulse approximation expressions requires knowledge of the struck nucleon's off shellness, i.e., the dependence of the nucleon structure function on the virtuality of the struck nucleon. Although a complete treatment of off-shell effects can only be given within a fully relativistic description of nuclear dynamics, model calculations exist which can estimate these corrections for DIS from both the deuteron and the complex nuclei. Off-shell effects can be described within a formalism which introduces corrections to the convolution formula of Eq. (8). However, as explained below, although their influence is felt mostly at large x, the ultimate effect on the extraction of the F_2^n/F_2^p ratio from the ratio $\mathcal{R}$ is rather small. Note that some authors write the flux factor $(1 + p_z/p_0)$ in Eq. (6) as $(1 + p_z/M)$ [46] or as $(p_0 + p_z)/M$ [45]. To the order in which we work, these are in fact equivalent and constitute small corrections numerically.

A further simplification of Eq. (8) can be made by observing that the nucleon momentum distributions $f(y)$ are strongly peaked about $y = 1$, so that by expanding the nucleon structure function about this point one can obtain approximate expressions for the nuclear structure functions in terms of average separation and kinematic energies. Keeping terms up to order p^2/M^2 (note that E is of order $p^2/2M$) one finds

$$F_2^A(x,Q^2) \approx F_2^N(x,Q^2) + x\frac{\partial F_2^N(x,Q^2)}{\partial x}\frac{\langle E\rangle + \langle T_R\rangle}{M} + x^2\frac{\partial^2 F_2^N(x,Q^2)}{\partial x^2}\frac{\langle T\rangle}{3M}, \tag{12}$$

where

$$\langle E\rangle = \int d^4p E \, S(p), \tag{13}$$

$$\langle T\rangle = \int d^4p \frac{\vec{p}^{\,2}}{2M} S(p), \tag{14}$$

$$\langle T_R\rangle = \int d^4p \frac{\vec{p}^{\,2}}{2M_{A-1}^*} S(p) \tag{15}$$

are the average separation, and kinetic and spectator recoil energies, respectively. Such an expansion will be useful in the following section in identifying the physical origin of the various contributions affecting the EMC ratios. For example, as we discuss in Sec. II E, the value of $\langle E\rangle$ determines the position of the peak in the function $f(y)$.

For the specific case of an $A = 3$ nucleus, calculation of the nuclear structure function amounts to determining the nucleon spectral function from the three-body nuclear wave function. The details are discussed in the following section, where we present two distinct and independent approaches: one by solving the homogeneous Faddeev equation with a given two-body interaction [47] and the other by using a variational technique [48,49]. In terms of the proton and neutron momentum distributions in ^{3}He, the nuclear structure function is given by

$$F_2^{^3\mathrm{He}} = 2 f_{p/^3\mathrm{He}} \otimes F_2^p + f_{n/^3\mathrm{He}} \otimes F_2^n . \tag{16}$$

Similarly for ^{3}H, the structure function is evaluated from the proton and neutron momentum distributions in ^{3}H:

$$F_2^{^3\mathrm{H}} = f_{p/^3\mathrm{H}} \otimes F_2^p + 2 f_{n/^3\mathrm{H}} \otimes F_2^n . \tag{17}$$

The proton and neutron distributions in ^{3}H can be related to those in ^{3}He according to

$$f_{n/^3\mathrm{H}} = f_{p/^3\mathrm{He}} + \Delta f_p \equiv f_p + \Delta f_p , \tag{18}$$

$$f_{p/^3\mathrm{H}} = f_{n/^3\mathrm{He}} + \Delta f_n \equiv f_n + \Delta f_n . \tag{19}$$

Because charge-symmetry breaking effects in nuclei are quite small, one can usually assume that $\Delta f_p \approx \Delta f_n \approx 0$, although in practice we consider both charge-symmetric and charge-symmetry breaking cases explicitly.

B. Three-nucleon spectral function

Calculations of the structure functions of $A=3$ nuclei can be performed by using realistic three-body spectral functions. In this section we first describe the relevant features of the spectral functions which determine the behavior of nuclear effects in DIS, following which we outline two different methods of computing the three-nucleon wave function, namely, via the Faddeev equations [47,50,51] and the variational approach [48,49].

To simplify the problem both theoretically and numerically, we will in the first instance consider the three-nucleon system with exact charge symmetry, so that both the ^{3}H and ^{3}He wave functions can be calculated simultaneously. The Coulomb interaction will of course modify the wave functions slightly through explicit charge-symmetry breaking effects, giving rise to the difference between ^{3}H and ^{3}He binding energies. We subsequently examine the effects of the binding energy on the structure functions.

The models we consider are based on two-body interactions. Possible three-body forces do not provide any significant improvement in the quality of the results, and are considerably more difficult to take into account. For the charge-symmetric case, one can treat ^{3}He and ^{3}H as members of an exact isospin doublet.

The nucleon spectral function is the joint probability of finding a nucleon in the nucleus A, with three-momentum $\vec{p}$ and removal energy E. If at the values of momentum and energy transfer considered the outgoing nucleon's motion is described by a plane wave, the spectral function can be written as the sum of the momentum densities for each final state:

$$S(p) = \frac{1}{(2\pi)^3} \sum_f \left| \int d^3 r e^{i\vec{p}\cdot\vec{r}} G_{fo}(\vec{r}) \right|^2 \delta(E - (E_2^f - E_3)), \tag{20}$$

where E_2^f and E_3 are the values of the total energy of the the two-nucleon spectator system and of the initial nucleus, respectively; $G_{fo}(\vec{r})$ is the overlap between the initial and final wave functions in coordinate space, with the $A-1$ (spectator) system being described in terms of a complete set of final states. The spectral function is normalized according to

$$\int d^4 p S(p) = 1. \tag{21}$$

Integrating the spectral function over the energy defines the nucleon momentum distribution in the nucleus:

$$\int dE S(p,E) = n(p). \tag{22}$$

There are, in general, two processes which can contribute to deep inelastic scattering from ^{3}He: (i) two-body breakup (with a deuteron d in the final state) and (ii) three-body breakup, pn and pp; analogously, for ^{3}H one has (i) two-body breakup (d) and (ii) three-body breakup, np and pp.

We write the spectral functions for the two nuclei, distinguishing between scattering from proton and neutron, as

$$S_{^3\mathrm{He}}(p) = \tfrac{2}{3} S_{p/^3\mathrm{He}}(p) + \tfrac{1}{3} S_{n/^3\mathrm{He}}(p), \tag{23}$$

$$S_{^3\mathrm{H}}(p) = \tfrac{1}{3} S_{p/^3\mathrm{H}}(p) + \tfrac{2}{3} S_{n/^3\mathrm{H}}(p), \tag{24}$$

where, in analogy with Eqs. (18) and (19), the proton and neutron spectral functions in ^{3}He and ^{3}H are related by

$$S_{p/^3\mathrm{He}}(p) = S_{n/^3\mathrm{H}}(p) \equiv S_p(p) + \Delta S_p(p), \tag{25}$$

$$S_{n/^3\mathrm{He}}(p) = S_{p/^3\mathrm{H}}(p) \equiv S_n(p) + \Delta S_p(p), \tag{26}$$

with the terms $\Delta S_{p,n}(p)$ representing explicit isospin symmetry breaking corrections.

By breaking down the spectral functions into contributions corresponding to two-body and three-body final states, one has

$$S_p(p) = S_p^{(2)}(p) + S_p^{(3)}(p), \tag{27}$$

$$S_n(p) \equiv S_n^{(3)}(p), \tag{28}$$

where $S_p^{(2)}$ and $S_p^{(3)}$ represent the contributions to the proton spectral function from a deuteron and the np breakup final states, while for the neutron spectral function only the pp final state contributes. In terms of these components, the average separation and kinetic energies can be written as

$$\langle E \rangle = \frac{2}{3} \int d^4 p [S_p^{(2)}(p) + S_p^{(3)}(p)] E + \frac{1}{3} \int d^4 p S_n(p) E$$

$$= \frac{2}{3} \langle E_p^{(2)} \rangle + \frac{1}{3} (2 \langle E_p^{(3)} \rangle + \langle E_n \rangle), \tag{29}$$

$$\langle T \rangle = \frac{2}{3} \int d^4 p [S_p^{(2)}(p) + S_p^{(3)}(p)] \frac{p^2}{2M} + \frac{1}{3} \int d^4 p S_n(p) \frac{p^2}{2M}$$

$$= \frac{2}{3} \langle T_p^{(2)} \rangle + \frac{1}{3} (2 \langle T_p^{(3)} \rangle + \langle T_n \rangle). \tag{30}$$

The normalization of the spectral function is written in terms of the normalizations for the two-body and three-body breakup spectral functions $\mathcal{N}_p^{(2)}$ and $\mathcal{N}_p^{(3)}$ as

$$1=\frac{2}{3}\int d^4p(S_p^{(2)}(p)+S_p^{(3)}(p))+\frac{1}{3}\int d^4pS_n(p)$$
$$=\frac{2}{3}(\mathcal{N}_p^{(d)}+\mathcal{N}_p^{(np)})+\frac{1}{3}. \tag{31}$$

In summary, we have shown the features of the spectral function $S(p)$ and of the light-cone function $f(y)$, which determine the behavior of the nuclear corrections to the deep inelastic structure functions at $x\geqslant 0.2$. While details of the short range structure could be important in determining the behavior at very large x, for $x\leqslant 0.6$–0.7 the nuclear modifications are determined by the values of the average removal and kinetic energies and, therefore, only loosely related to the detailed structure of the spectral function. Thus, we can safely state that nuclear effects are under control.

Having developed the formalism, in the following we describe the evaluation of the spectral function, within the Faddeev and variational approaches, from which the nuclear structure function will be calculated.

1. Faddeev equations

A full description of the calculation of the Faddeev wave function used here has been given in Ref. [47]. We therefore only briefly outline the calculation here. We work in momentum space using a separable potential, which further simplifies the computation [52]. The wave function is written as a sum of so-called ''Faddeev components'' [53,54]:

$$|\Psi\rangle=|\varphi_\alpha\rangle+|\varphi_\beta\rangle+|\varphi_\gamma\rangle=\{e+(\alpha\beta\gamma)+(\alpha\gamma\beta)\}|\varphi_\gamma\rangle, \tag{32}$$

where α, β, and γ are indices running from 1 to 3 (with $\alpha\neq\beta\neq\gamma$). In this equation ''$e$'' is the neutral element of the permutation group of three objects, and ''$(\alpha\beta\gamma)$'' and ''$(\alpha\gamma\beta)$'' are cyclic permutations. $|\varphi_\alpha\rangle$ is referred to as the ''Faddeev component'' of the wave function in which the spectators to the nucleon α interact last [55].

Using the symmetry properties of the wave function (see, e.g., Refs. [47,54]), one writes a set of coupled equations for the Faddeev components:

$$|\varphi_\alpha\rangle=G_0t_\alpha(|\varphi_\beta\rangle+|\varphi_\gamma\rangle), \tag{33}$$

where t_α is the usual t matrix defined by the Lippmann-Schwinger equation:

$$t_\alpha(E)=V_\alpha+V_\alpha G_0(E)t_\alpha(E)=(1-G_0(E)V_\alpha)^{-1}V_\alpha, \tag{34}$$

with $G_0(E)=(E-H_0)^{-1}$ and V_α the interaction between particles β and γ. From these expressions one can derive a set of homogeneous Faddeev equations for the spectator function Ξ [56],

$$\Xi_{N_\alpha}(p_\alpha)=2\sum_{N'_\alpha N_\beta}\tau_{N_\alpha N'_\alpha}(E,p_\alpha)\int_0^{+\infty}dp_\beta p_\beta^2$$
$$\times\mathcal{Z}_{N'_\alpha N_\beta}(E,p_\alpha,p_\beta)\Xi_{N_\beta}(p_\beta), \tag{35}$$

where $\mathcal{Z}$ is the kernel of the integral equation, and the matrix $\tau_{N_\alpha N'_\alpha}$ is related to the t matrix by

$$t_{n_\alpha n'_\alpha}(E)=|g_{n_\alpha}\rangle\tau_{n_\alpha n'_\alpha}(E)\langle g_{n'_\alpha}|. \tag{36}$$

Here, a three-nucleon channel is denoted by an index N_α and a two-nucleon channel by an index n_α. The form factor g_{n_α} is defined by the form of the separable potential. Details of the computation of the τ matrix and the kernel are given in Refs. [54,57] and [47,57,58], respectively.

The relevance of the spectator function becomes clear if one considers the relation between Ξ and φ_α:

$$\langle\Omega_{N_\alpha}^{JI}|\varphi_\alpha\rangle=2G_0(E)|g_{N_\alpha}\rangle|\Xi_{N_\alpha}\rangle, \tag{37}$$

where $|\Omega_{N_\alpha}^{JI}\rangle$ is the angular element of our partial wave decomposition for isospin I and spin J. The homogeneous equation (35) then enables one to compute the contribution from one of the Faddeev components to the total wave function. The total wave function relative to the decomposition in the $|\Omega_{N_\alpha}^{JI}\rangle$ partial wave also requires the contributions $\langle\Omega_{N_\alpha}^{JI}|\varphi_\beta\rangle$ and $\langle\Omega_{N_\alpha}^{JI}|\varphi_\gamma\rangle$. Since one has a system of identical particles, these two contributions are equal for obvious reasons of symmetry. Details of the computation of this contribution can be found in Ref. [47].

To examine the model dependence of the distribution function we use several different potentials, namely, the ''EST'' (Ernst-Shakin-Thaler) separable approximation to the Paris potential [59] (referred to as ''PEST''), the unitary pole approximation [60] to the Reid soft core (RSC) potential [61], and the Yamaguchi potential [62] with 7% mixing between $^3S_1$ and $^3D_1$ waves. The homogeneous Faddeev equation was solved with five channels for both potentials. The results for the trinucleon binding energies are -7.266 MeV (PEST) and -8.047 MeV (Yamaguchi), which differ by $\sim 14\%$ and $\sim 5\%$, respectively, from the experimental ^{3}H binding energy of -8.482 MeV (one expects the binding energy from this trinucleon calculation to be closer to the experimental ^{3}H binding energy than ^{3}He, since one does not expect Coulomb corrections for ^{3}H).

The issue of the binding energy is well known, and this result is consistent with what one usually expects when the Coulomb interaction is switched off. To estimate the effect of neglecting the Coulomb interaction in ^{3}He and at the same time correct the long range part of the three-body wave function due to the change in the binding energy, we have modified the $^1S_0$ potential in ^{3}He and ^{3}H to reproduce their respective experimental energies. This leaves the $^3S_1$–$^3D_1$ interaction responsible for the formation of the deuteron unchanged, and introduces a rather strong charge-symmetry breaking in the system. This approximation distributes the symmetry breaking effects of the Coulomb interaction

equally over the three particles, whereas in the exact case it should only arise from the difference between pp and np interactions. It therefore represents an overestimate of any charge-symmetry breaking effects, since one attributes to charge-symmetry breaking an effect which should partly come from three-body forces. However, this simple modification to the $^1S_0$ interaction will allow us to study explicitly the possible effects on the deep inelastic structure functions associated with the differences in the binding energies of ^{3}He and ^{3}H.

2. Variational approach

In the variational approach one writes the overlap integral in coordinate space, $G_{fo}(\vec{r})$, Eq. (20), as

$$G_{fo}(\vec{r}) = \mathcal{N} \int d^3\vec{\rho}\, \psi_2^f(\vec{\rho})\, \psi_3^i(\vec{r},\vec{\rho}), \tag{38}$$

where $\mathcal{N}$ is a normalization factor; $\psi_2^f(\vec{\rho})$ and $\psi_3^i(\vec{r},\vec{\rho})$ are the wave functions with eigenvalue E_2^f for the spectator two-body system and with eigenvalue E_3 for the initial three-body system, respectively; $f \equiv (J_f, M_f, S_f, \lambda)$ represents the quantum numbers of the spectator system, λ specifying the tensor coupled states at high energy and momentum and $i \equiv (1/2, M)$; and $\vec{r}$ and $\vec{\rho}$ are the intrinsic coordinates for the three body system [63].

The three-body wave function is found by diagonalization of the intrinsic nuclear Hamiltonian using an LS coupling scheme, and the basis

$$|\phi_K\rangle = |(Ll)L, (S\tfrac{1}{2})S; \tfrac{1}{2}M\rangle, \tag{39}$$

where L and l refer to two sets of harmonic oscillator wave functions with different harmonic oscillator parameters [64]. The wave function is then written schematically as

$$\psi_3^i(\vec{r},\rho) = \sum_K |\phi_K\rangle, \tag{40}$$

where the relevant components are the ones with $L=0$ and $L=2$. All calculations using the variational method outlined here have been performed using the RSC [61] interaction.

The two-body spectator wave function describes either a deuteron, $\psi_2^f(\vec{r}) \equiv \psi_d(\vec{r})$ (two-body channel) or an interacting nucleon pair (three-body channel). The corresponding quantum numbers and ground state energy values are $f \equiv (1, M_J, 1)$ and $E_2^f = -2.23$ MeV (two-body channel); $f \equiv (J, M_J, S, \lambda)$ and $E_2^f > 0$ (three-body channel). The three-body channel wave function calculated in Ref. [49] considers states up to $J=5$, using the RSC interaction up to $J=2$. For higher values of J, the interaction among the two nucleons is assumed to be negligible.

Analogous issues, such as for the Faddeev calculations outlined above, are present in the variational approach, namely, discrepancies in the theoretical values of the binding energy depending on the type of potential, the accurate handling of Coulomb effects, and the possible presence of charge-symmetry breaking effects. These issues are examined quantitatively in Sec. IV.

C. Nucleon momentum distributions

Before proceeding to the evaluation of the structure functions in terms of the nuclear spectral functions, we first review some general features of the spectral functions and light-cone momentum distribution $f(y)$.

The relevant features of the ^{3}He spectral function are given as follows.

(i) A pronounced peak at $E=2$ MeV, corresponding to the case in which the spectator deuteron recoils.

(ii) Some strength extending to high values of the energy and momentum ($p \gtrsim 300$ MeV), but lying at least three orders of magnitude below the peak. The high momentum and energy part of the spectral function is given almost entirely by the short range part of the nucleon-nucleon interaction which is actually responsible for breakup configurations of the spectator system. In heavier nuclei these components can be calculated using two-nucleon correlations, as described by Ciofi degli Atti *et al.* [65].

The function $f(y)$ reflects the features of the spectral function described above. Namely, it has a sharp peak in the vicinity of $y=1$, $y_{\rm peak} \approx 1 - \langle E \rangle / M$ (modulo spectator recoil corrections, see below), and some strength away from $y_{\rm peak}$ is present which integrates to a considerable fraction of the total strength. For the proton, all the distributions have a similar shape and peak value, however, for the neutron the variational distribution peaks at slightly smaller y and has a larger tail than the Faddeev. The origin of this is the larger momentum components in the deuteron spectator part of the neutron distribution in the variational distribution than in the corresponding Faddeev distribution.

The main contribution of $f(y)$ in the convolution formula is from its values around $y_{\rm peak}$, namely, one can write

$$F_2^A(x,Q^2) \approx F_2^N(x/y_{peak}, Q^2) < F_2^N(x,Q^2). \tag{41}$$

Since F_2^N is a decreasing function of x in the interval $0.2 \lesssim x \lesssim 0.6$, this gives rise to the depletion in the EMC ratio, F_2^A/F_2^N. At larger x, the EMC ratio rises above unity because of the different kinematic boundaries affecting the smearing; namely, using the asymptotic convolution formula, the kinematic thresholds for the free nucleon, the deuteron, and $A=3$ nuclei are located at $x=1$, $x=2$, and $x=3$, respectively.

In summary, the EMC effect at intermediate values of x ($0.2 \leqslant x \leqslant 0.65$) is determined almost entirely by the average values of the removal and kinetic energies, Eq. (41) and Eq. (12). At larger values of x, the approximations Eq. (41) and Eq. (12) start breaking down, and the EMC effect is directly sensitive to the large energy and momentum components of the spectral function.

Note also that $f(y)$ can be translated easily into the "Y-scaling" function $F(Y)$ [66], extracted from quasielastic scattering. The variable Y is given in terms of y and the nucleon and nuclear masses as $Y = (1/2)[M_A - My)^2 - M_{A-1}^2]/(M_A - My)$, which allows one to relate $F(Y)$

$=f(y)/M$. Unlike in DIS, the nuclear cross sections for quasielastic scattering are given directly in terms of $f(y)$, so that quasielastic data can be used in addition to constrain models of nuclear dynamics. A quantitative description, however, of quasielastic scattering requires additional contributions beyond the impulse approximation, such as from meson-exchange currents, which do not contribute in deep inelastic scattering. In our analysis we use distributions which are consistent with those used in standard analyses of quasielastic scattering data.

D. EMC effect in $A=3$ nuclei

Before proceeding to the calculation of the ratio $\mathcal{R}$ of the EMC effects in ^{3}He and ^{3}H, and the associated sensitivity of the extracted F_2^n/F_2^p to $\mathcal{R}$, we first discuss the predictions of the conventional nuclear models for the absolute EMC ratios and compare with available data.

As well as offering a relatively clean way to extract F_2^n from nuclear data, the $A=3$ system is also a valuable laboratory for testing models of the EMC effect for few-body nuclei. Although the determination of F_2^n/F_2^p requires only the ratio of ^{3}He to ^{3}H structure functions, data on the absolute values of $F_2^{^3\mathrm{He}}$ and $F_2^{^3\mathrm{H}}$ can in addition fix the magnitude of the EMC effect in $A=3$ nuclei:

$$R(^3\mathrm{He}) = \frac{F_2^{^3\mathrm{He}}}{F_2^p(2+F_2^n/F_2^p|_{\mathrm{extr}})}, \tag{42}$$

$$R(^3\mathrm{H}) = \frac{F_2^{^3\mathrm{H}}}{F_2^p t(1+2F_2^n/F_2^p|_{\mathrm{extr}})}. \tag{43}$$

Unfortunately, at present there are no data at all on the $F_2^{^3\mathrm{H}}$ structure function, and only scant information on $F_2^{^3\mathrm{He}}$ is available, from a recent HERMES measurement [17], the main focus of which was the low-x, low-Q^2 region. Nevertheless, the available data can provide a useful check on the calculation.

In Fig. 2 the ratio of the ^{3}He to free-nucleon (corrected for nonisoscalarity) structure functions is shown for the Faddeev (PEST) and variational wave functions, compared with the HERMES data [17] on the ratio of $\sigma(^3\mathrm{He})/[\sigma(d)+\sigma(p)]$. The difference between the solid and dashed curves in Fig. 2 illustrates the effect on the ratio due to possible nuclear corrections in deuterium. The various models predict qualitatively similar behavior for the ratio as a function of x, with the magnitude of the depletion at $x\sim 0.5-0.7$, ranging from $\sim$2% in the variational approach to $\sim$4% using the Faddeev wave functions. Within the relatively large errors for $x\gtrsim 0.4$, the agreement between the models and the experiment is reasonably good.

A similar behavior is found for the ratio of ^{3}H to isoscalar nucleon structure functions, illustrated in Fig. 3 for the Faddeev and variational calculations. The trough at $x\sim 0.6$ in ^{3}H is predicted to be slightly deeper than that in ^{3}He in all models. The dependence on the input potential is negligible, as the PEST and RSC Faddeev results illustrate. Data on ^{3}H, and better quality data extending to larger x for ^{3}He, would clearly be of great value in constraining models of the EMC effect in $A=3$ nuclei.

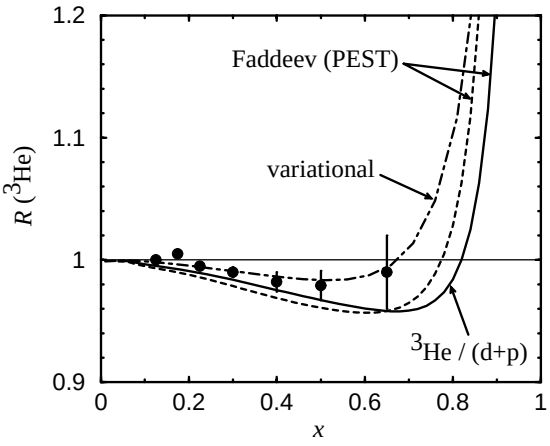

FIG. 2. Nuclear EMC ratio in ^{3}He using the Faddeev (with the PEST potential) and variational (RSC) wave functions, compared with HERMES data [17] for $\sigma(^3\mathrm{He})/[\sigma(d)+\sigma(p)]$. The solid curve corresponds to $F_2^{^3\mathrm{He}}/(F_2^d+F_2^p)$, while the dashed and dot-dashed assume no EMC effect in the deuteron.

IV. RATIO OF RATIOS

In this section we discuss the model dependence of the ratio $\mathcal{R}$ of the ^{3}He and ^{3}H EMC ratios arising from uncertainty in the nuclear wave function, the off-shell modifications of the nucleon structure function, and possible non-nucleonic degrees of freedom in the $A=3$ nuclei. While the magnitude of the EMC effect in ^{3}He and ^{3}H was found in the preceding section to differ by as much as several percent at $x\lesssim 0.8$ in different models, one expects the ratio of these to be considerably less model dependent.

A. Nuclear wave function dependence

Using the light-cone momentum distributions described in Sec. III, the ratio $\mathcal{R}=R(^3\mathrm{He})/R(^3\mathrm{H})$ of EMC ratios for ^{3}He

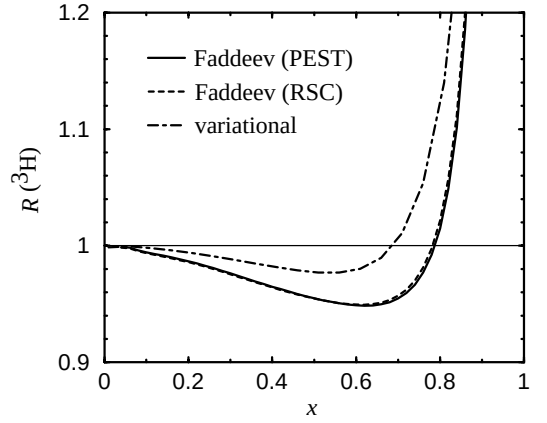

FIG. 3. Nuclear EMC ratio in ^{3}H using the Faddeev (with PEST and RSC potentials) and variational (RSC) wave functions.

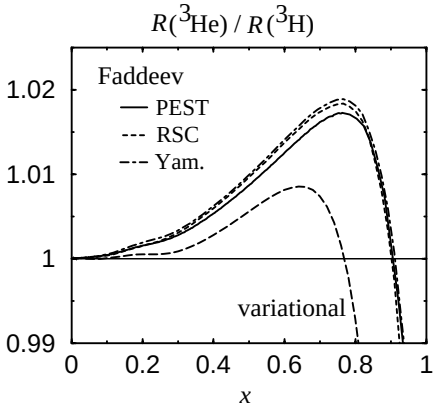

FIG. 4. Ratio $\mathcal{R}$ of nuclear EMC ratios for ^{3}He and ^{3}H nuclei, with the nucleon momentum distribution calculated from the Faddeev (PEST, RSC, and Yamaguchi) and variational (RSC) wave functions.

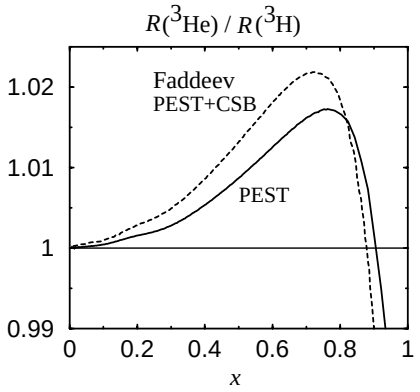

FIG. 5. Ratio of nuclear EMC ratios for ^{3}He and ^{3}H for the Faddeev (PEST) wave function, with (dashed) and without (solid) charge-symmetry breaking (CSB) effects.

to ^{3}H is shown in Fig. 4 for various nuclear model wave functions, namely, Faddeev with the PEST, RSC, and Yamaguchi potentials, and variational using the RSC potential. (Unless otherwise stated, in all cases the CTEQ5 parametrization [67] of parton distributions at $Q^2=10$ GeV^2 will be used for F_2^N.) The EMC effects are seen to mostly cancel over a large range of x, out to $x\sim 0.8$, with deviation from a "central value" $\mathcal{R}\approx 1.01$ to within $\pm 1\%$. The larger absolute EMC effects in ^{3}He and ^{3}H predicted with the Faddeev calculations in Figs. 2 and 3 are reflected in a larger deviation of $\mathcal{R}$ from unity than with the variational wave functions, as seen in the three Faddeev calculations in Fig. 4. Furthermore, the dependence on the NN potential is very weak. In practice, the exact shape of $\mathcal{R}$ will not be important for the purposes of extracting F_2^n/F_2^p from the $F_2^{^3\mathrm{He}}/F_2^{^3\mathrm{H}}$ ratio; rather, it is essential that the model dependence of the deviation of $\mathcal{R}$ from the central value should be small.

B. Charge-symmetry breaking

The ratio $\mathcal{R}$ in Fig. 4 was calculated using three-nucleon wave functions neglecting the Coulomb interaction and working in an isospin basis [68]. To estimate the effect of neglecting the Coulomb interaction in ^{3}He and at the same time correct the long range part of the three-body wave function due to the change in the binding energy, we modify the $^1S_0$ potential in the ^{3}He and ^{3}H to reproduce their respective experimental energies. In this way, the $^3S_1$-$^3D_1$ interaction responsible for the formation of the deuteron is unchanged. This approximation spreads the effect of the Coulomb interaction over both the pp and the np interaction in the $^1S_0$ channel. To this extent, it shifts some of the Coulomb effects in the neutron distribution in ^{3}He to the proton distribution. However, this simple modification to the $^1S_0$ interaction allows one to study explicitly the possible effects associated with the differences in the binding energies of ^{3}He and ^{3}H.

The ratio $\mathcal{R}$ calculated with the Faddeev (PEST) wave function modified according to this prescription is shown in Fig. 5 (dashed curve), compared with the charge-symmetric result (solid). The effect of this modification is a shift of $\lesssim 0.5\%$ in $\mathcal{R}$, maximal at $x\sim 0.65$. The effects of charge-symmetry breaking therefore still leave a ratio which deviates from unity by $\lesssim 2\%$.

C. Finite Q^2 effects

The structure function ratios discussed above are calculated assuming leading twist dominance of the nucleon structure function at $Q^2=10$ GeV^2. At finite Q^2 there will be contributions from both the kinematic factor $\mathcal{F}$ in the inelastic structure function, Eq. (6), and from higher twist ($\propto 1/Q^2$) effects, including quasielastic scattering from the bound nucleon, which may not be negligible at large x [69]. To illustrate the impact of these finite-Q^2 effects on the ratio $\mathcal{R}$, in Fig. 6 we show the ratio at several values of Q^2 ($Q^2=4$ GeV^2 and 20 GeV^2) together with the asymptotic result ($\mathcal{F}\to 1$). To facilitate the comparison, all curves have been

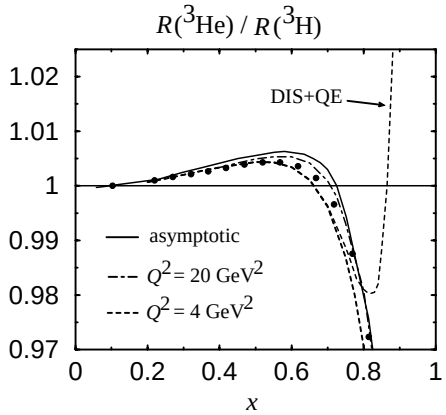

FIG. 6. Q^2 dependence of the ratio $\mathcal{R}$ of ^{3}He and ^{3}H nuclear EMC ratios for the variational wave functions with the RSC potential. Results using the full Q^2 dependence in Eq. (6) at $Q^2=4$ GeV^2 (dashed) and $Q^2=20$ GeV^2 (dot-dashed) are compared with the asymptotic prediction (solid), and at varying Q^2 (filled circles) ranging from $Q^2=3$ GeV^2 for the lowest x bin to $Q^2=14$ GeV^2 at the highest-x bin. The effect of the quasielastic contribution (DIS+QE) at $Q^2=4$ GeV^2 is also indicated.

obtained using the variational $A=3$ wave functions. The points denoted by bullets correspond to values of x and Q^2 that would be relevant for kinematics at a 12-GeV Jefferson Lab facility [13] (see Sec. V and Table I below), for which Q^2 varies from $Q^2=3$ GeV^2 in the lowest-x bin to $Q^2=14$ GeV^2 in the highest-$x(\approx 0.8)$ bin. The effect of the Q^2 dependence is clearly rather modest.

The role of quasielastic scattering is illustrated by the dashed curve in Fig. 6 for $Q^2=4$ GeV^2. For $x \lesssim 0.8$, the quasielastic contribution is negligible for the relevant kinematics, with a correction of the order of 1% at $x=0.8$. At the largest values of x, for instance, where $Q^2=14$ GeV^2, we have checked that the quasielastic contribution is suppressed. Its effect does start to become important, however, for $x \gtrsim 0.85$ at fixed $Q^2 \lesssim 5$ GeV^2, as can be seen from the wiggle produced in the dashed curve in Fig. 6.

To test the sensitivity of $\mathcal{R}$ to higher twist corrections, we compute the ratio using the fit to the total F_2 structure function from Donnachie and Landshoff (DL) [70], which includes both leading and subleading effects in $1/Q^2$. The difference between the leading twist only and the leading plus higher twist (HT) curves, represented by the lower and upper dashed curves in Fig. 7 ["DL" and "DL(HT)," respectively], is negligible for $x \lesssim 0.8$, increasing to $\sim 1\%$ at $x \sim 0.85$. The size of the higher twist corrections can be determined by taking measurements at several values of Q^2 and observing any $1/Q^2$ dependence of the structure function. In particular, since the Q^2 dependence of F_2^p has been measured in a number of earlier experiments [71], the Q^2 dependence of the extracted F_2^n/F_2^p ratio can be used to separate the leading twist from the nonleading twist components of F_2^n [72].

D. Iteration procedure

The dependence of $\mathcal{R}$ on different input nucleon structure function parametrizations is illustrated in Fig. 7, where several representative parton distribution function fits are given at $Q^2=10$ GeV^2. Apart from the standard CTEQ fit (solid), the results for the GRV [73] (dot-dashed), DL [70] (dashed), and BBS [74] (dotted) parametrizations are also shown (the latter at $Q^2=4$ GeV^2). For $x \lesssim 0.6$, there is little dependence ($\lesssim 0.5\%$) in the ratio on the structure function input. For $0.6 \lesssim x \lesssim 0.85$ the dependence is greater, but still with $\lesssim \pm 1\%$ deviation away from the central value $\mathcal{R} \approx 1.01$. The spread in this region is due mainly to the poor knowledge of the neutron structure function at large x. Beyond $x \approx 0.85$ there are few data in the deep inelastic region on either the neutron or proton structure functions, so here both the d and u quark distributions are poorly determined.

A standard assumption in most global fits of parton distributions is that $d/u \to 0$ as $x \to 1$. This assumption has recently been questioned on theoretical and phenomenological grounds [6,9]. The BBS parametrization [74], on the other hand, incorporates constraints from perturbative QCD, and forces $d/u \to 0.2$ as $x \to 1$ [23]. The effect of the different large-x behavior of the d quark is apparent only for $x \gtrsim 0.85$, where it gives a difference of ~ 1–2% in $\mathcal{R}$ compared with the fits in which $d/u \to 0$. One can also modify the standard CTEQ fit, for example, by applying a correction factor [9] to enforce $d/u \to 0.2$. However, this also produces differences in $\mathcal{R}$ which are $\lesssim 2\%$ for $x < 0.9$.

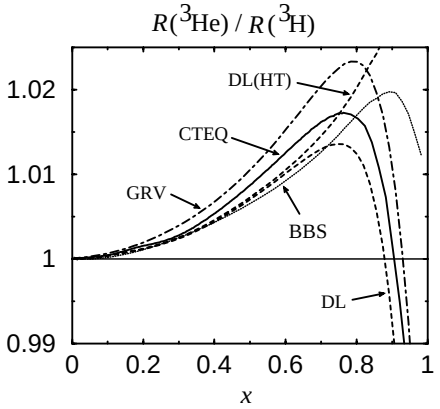

FIG. 7. Ratio of nuclear EMC ratios for ^{3}He and ^{3}H with the the Faddeev (PEST) wave functions, for various nucleon structure function parametrizations: CTEQ [67], GRV [73], BBS [74], and DL [70] with leading twist only, and with higher twist (HT) correction.

Despite the seemingly strong dependence on the nucleon structure function input at very large x, this dependence is actually artificial. In practice, once the ratio $F_2^{^3\mathrm{He}}/F_2^{^3\mathrm{H}}$ is measured, one can employ an iterative procedure to eliminate the dependence altogether [14,75,76]. Namely, after extracting F_2^n/F_2^p from the data using some calculated $\mathcal{R}$, the extracted F_2^n can then be used to compute a new $\mathcal{R}$, which is then used to extract a new and better value of F_2^n/F_2^p. This procedure is iterated until convergence is achieved and a self-consistent solution for the extracted F_2^n/F_2^p and $\mathcal{R}$ is obtained. The results of this procedure are shown in Fig. 8 for different numbers of iterations using as input $F_2^n/F_2^p=1$. The convergence is relatively rapid—by the third iteration the extracted function is almost indistinguishable from the exact result. Although the effect on $\mathcal{R}$ from the present lack of knowledge of the nucleon structure function is $\lesssim 2\%$ for $x \lesssim 0.85$, this uncertainty can in principle be eliminated altogether via iteration, so that the only model dependence of $\mathcal{R}$ will be from the nuclear interaction in the $A=3$ nucleus.

Of course, the accuracy of the iteration procedure is only as good as the reliability of the formalism in Sec. III used to calculate the nuclear structure functions. As pointed out in Ref. [77], large corrections to the smearing expression (6) could lead to inaccuracies in the extracted F_2^n/F_2^p ratio. In particular, it was argued [77] that strong isospin-dependent off-shell effects could give significantly larger deviations of $\mathcal{R}$ from unity than that found in Refs. [14,75]. In the following we shall carefully examine the issue of off-shell effects in $A=3$ nuclei and their effect on the $\mathcal{R}$ ratio.

E. Nucleon off-shell deformation

The derivation of the convolution approximation in Eq. (8) assumes that the nucleon off-shell dependence in the bound nucleon structure function in Eq. (6) is negligible. In

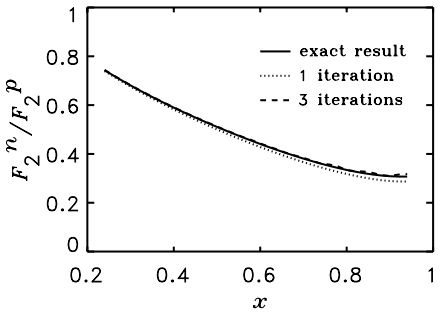

FIG. 8. Neutron to proton structure function ratio extracted from the $F_2^{^3\mathrm{He}}/F_2^{^3\mathrm{H}}$ ratio via the iteration procedure. The input is $F_2^n/F_2^p=1$, and the ratio after ~ 3 iterations is indistinguishable from the exact result.

this section, we examine the accuracy of this assumption. The off-shell dependence of F_2^N is, as a matter of principle, not measurable, since one can always redefine the nuclear spectral function to absorb any p^2 dependence in the bound nucleon structure function. However, off-shell effects can be identified once a particular form of the interaction of a nucleon with the surrounding nuclear medium is specified. The discussion of off-shell modification of the nucleon structure function in the nuclear medium is therefore understood to be within the framework of the nuclear spectral functions defined in Sec. III.

In convolution models, off-shell corrections can arise both kinematically, through the transverse motion of the nucleon in the nucleus, and dynamically, from modifications of the bound nucleon's internal structure. Kinematical off-shell effects are essentially model independent, as discussed in Ref. [35], while dynamical off-shell effects do depend on descriptions of the intrinsic deformation of the bound nucleon structure and are therefore model dependent. The latter have been modeled, for instance, in a covariant spectator model [33], in which the DIS from a bound nucleon is described in terms of relativistic vertex functions which parametrize the nucleon-quark-spectator ''diquark'' interaction. The dependence of the vertex functions on the quark momentum and the diquark energy is constrained by fitting to the on-shell nucleon (proton) structure function data, while the additional dependence on the virtuality of the off-shell nucleon can be constrained by comparing the calculated nuclear structure function with the inclusive F_2^A data.

Taking the nucleon's off-shellness into account, the bound nucleon structure function in Eq. (8) can be generalized to [33,35,46]

$$F_2^A(x,Q^2)=\int dy \int dp^2 \varphi(y,p^2,Q^2) F_2^N(x',p^2,Q^2), \tag{44}$$

where $x'=x/y$ and the function $\varphi(y,p^2,Q^2)$ depends on the nuclear wave functions. In the absence of p^2 dependence in F_2^N, the light-cone momentum distribution $f(y,Q^2)$ in Eq. (8) would correspond to the p^2 integral of $\varphi(y,p^2,Q^2)$. In the approach of Ref. [35], the medium modified nucleon structure function $F_2^N(x',p^2,Q^2)$ can be evaluated in terms of a relativistic quark spectral function ρ_N as

$$F_2^N(x',p^2,Q^2)=\frac{x'^2}{1-x'}\sum_X \int_{k^2_{\min}} \frac{dk^2}{4(2\pi)^3}\rho_N(k^2(p),p_X^2), \tag{45}$$

where ρ_N depends on the virtualities of the struck quark, k^2, and spectator system, p_X^2, and the limit $k_{\min}=k_{\min}(x',p^2,p_X^2)$ follows from the positivity constraint on the struck quark's transverse momentum $k_\perp^2 \geqslant 0$. The dependence of $k_{\min}$ on p^2 $(\neq M^2)$ generates an off-shell correction which grows with A due to the A dependence of the virtuality p^2 of the bound nucleon. This serves to enhance the EMC effect at large x in comparison with naive binding model calculations which do not take into account nucleon off-shell effects [45]. Assuming that the spectator quarks can be treated as a single system with a variable mass m_X^2, the off-shell structure function in Eq. (45) can be related to the on-shell function by a p^2-dependent rescaling of the argument x', namely [35],

$$F_2^N(x')|_{p^2\neq M^2} \rightarrow F_2^N(x'(p^2)>x')|_{p^2=M^2}. \tag{46}$$

It is this (further) rescaling in x that is responsible for the larger effect at large x.

The effect of the off-shell correction on the ratio $\mathcal{R}$, illustrated in Fig. 9, is a small ($\lesssim 1\%$) increase in the ratio at $x \sim 0.6$. Off-shell effects of this magnitude can be expected in models of the EMC effect where the overall modification of the nuclear structure function arises from a combination of conventional nuclear physics phenomena associated with nuclear binding, and a small medium dependence of the nucleon's intrinsic structure [1,33,46,78].

Other models of the EMC effect, such as the color screening model for suppression of pointlike configurations (PLC) in bound nucleons [79], attribute most or all of the EMC effect to a medium modification of the internal structure of the bound nucleon, and consequently predict larger deviations of $\mathcal{R}$ from unity [77]. However, recent $^4\mathrm{He}(\vec{e},e'\vec{p})$ polarization transfer experiments [80] indicate that the magnitude of the off-shell deformation is indeed rather small. The measured ratio of transverse to longitudinal polarization of the ejected protons in these experiments can be related to the medium modification of the electric to magnetic elastic form factor ratio. Using model-independent relations derived from quark-hadron duality, the medium modifications in the form factors were related to a modification at large x of the deep inelastic structure function of the bound nucleon in Ref. [81]. In ^{4}He, for instance, the effect in the PLC suppression model was found [81] to be an order of magnitude larger than that allowed by the data [80], and with a different sign for $x \gtrsim 0.65$. The results therefore place rather strong constraints on the size of the medium modification of the structure of the nucleon, suggesting little room for large off-shell corrections, and support a conventional nuclear physics description of the ^{3}He/^{3}H system as a reliable starting point for nuclear structure function calculations.

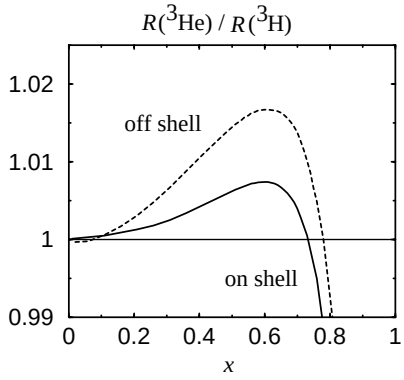

FIG. 9. Ratio $\mathcal{R}$ of nuclear EMC ratios for ^{3}He and ^{3}H nuclei, with (dashed) and without (solid) nucleon off-shell corrections [35] (see text), for the variational (RSC) wave function.

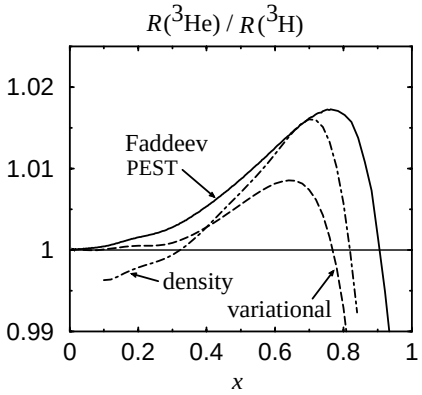

FIG. 10. Ratio of nuclear EMC ratios for ^{3}He and ^{3}H for the density extrapolation model, compared with the standard Faddeev (PEST) and variational (RSC) wave functions.

F. Nuclear density extrapolation model

The nuclear density model, which has proven successful for studying the A dependence of the EMC effect for heavy nuclei, stems from the empirical observation that for heavy nuclei the deviation from unity in the EMC ratio $R(A)$ is assumed to scale with nuclear density [4]:

$$\frac{R(A_1)-1}{R(A_2)-1}=\frac{\rho(A_1)}{\rho(A_2)}, \tag{47}$$

where $\rho(A)=3A/(4\pi R_A^3)$ is the mean nuclear density and $R_A^2=(5/3)\langle r^2\rangle_A$. Whether the concept of density is physically meaningful for a few-body system such as a ^{3}He nucleus is rather questionable [82]. However, one can use the density extrapolation ansatz to investigate the range of predictions for $\mathcal{R}$, and estimate the total theoretical uncertainty.

From the empirical $A=3$ charge radii [83], one finds that $\rho(^3\mathrm{H})/\rho(^3\mathrm{He})\approx 140\%$, so that the EMC effect in ^{3}H is predicted to be 40% larger than in ^{3}He. However, as shown in Fig. 10, assuming that $R(^3\mathrm{He})$ can be extrapolated from the measured EMC ratios for heavy nuclei such as ^{56}Fe, one still finds that the ratio $|\mathcal{R}-1|<2\%$ for all $x\lesssim 0.85$. The x dependence predicted by density extrapolation method lies approximately between that using the standard Faddeev and variational techniques for $0.5\lesssim x\lesssim 0.85$.

G. Six-quark clusters

While most of the medium modification of the nuclear structure function at large x can be described in terms of incoherent scattering from bound nucleons, other effects involving explicit quark degrees of freedom have been suggested as possible sources of EMC-type modifications. In particular, at short nucleon-nucleon separations the effects of quark exchange could be more prominent. Corrections to the impulse approximation arising from the exchange of quarks between nucleons in $A=3$ nuclei were in fact discussed in Ref. [84] (see also Ref. [85]). There the effect on the EMC ratio, for the isospin-averaged $A=3$ nucleus, was found to be comparable to that arising from binding. However, the analysis [84] did not allow for NN correlations, which are important at large momentum (and hence large x), so that the overall EMC effect is likely to have been overestimated.

The effects of quarks which are not localized to single nucleons can alternatively be parametrized in terms of multiquark clusters, in which six (or more) quarks form color singlets inside nuclei [86]. Six-quark configurations in the deuteron and other nuclei have been studied in a variety of observables, including nuclear electromagnetic form factors, NN scattering, as well as the EMC effect. To test the possible role of quark exchange on the ratio $\mathcal{R}$, we consider the effect of six-quark clusters on ^{3}He and ^{3}H structure functions (contributions from nine-quark clusters are presumably small compared with those from six-quark states). Although neither the normalization of the six-quark component of the $A=3$ wave function nor its momentum distribution is known,one can nevertheless estimate their potential importance by examining the effect on $\mathcal{R}$ for a range of parameters.

Following Ref. [86], contributions from scattering off quarks in a six-quark cluster can be approximated by an effective six-quark structure function $F_2^{6q}(x_{6q})$ in the nucleus, where $x_{6q}=Q^2/2M_{6q}\nu\approx x/2$. If P_{6q} is the probability of finding a six-quark cluster in the nucleus, the net effect on the ^{3}He (and similarly ^{3}H) structure function can be approximated by

$$F_2^{^3\mathrm{He}}\to(1-P_{6q})F_2^{^3\mathrm{He}}+P_{6q}F_2^{6q}, \tag{48}$$

where $F_2^{^3\mathrm{He}}$ is the incoherent nucleon contribution. Taking a typical valence-like shape for F_2^{6q}, with the large-x behavior constrained by hadron helicity counting rules, $F_2^{6q}\sim(1-x_{6q})^9$, the effect on $\mathcal{R}$ is shown in Fig. 11 for $P_{6q}=0\%$, 2%, and 4%. The overall effect is $\lesssim 1\%$ for all $x\lesssim 0.85$ even for the largest six-quark probability considered. For larger values of P_{6q} deviation from unity is in fact even smaller, canceling some of the effects associated with nucleon off-shell dependence, for instance. We have also considered other six-quark structure functions, and while there is some sensitivity to the exact shape of F_2^{6q}, the $\sim 1\%$ effect on $\mathcal{R}$ appears to be an approximate upper limit for all x.

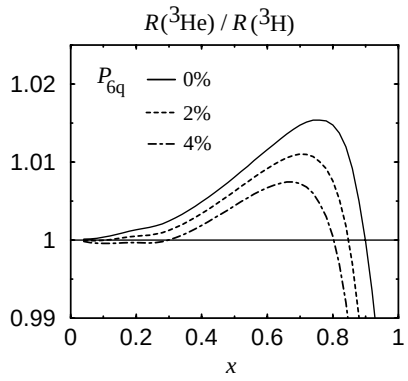

FIG. 11. Ratio of nuclear EMC ratios for ^{3}He and ^{3}H for the Faddeev (PEST) wave function, with $P_{6q}=0\%$, 2%, and 4% six-quark configurations in the $A=3$ wave function.

V. EXPERIMENTAL CONSIDERATIONS

Measurements of the nucleon structure functions have been performed at several accelerator laboratories over the past 35 years. The highest-x measurements using proton and deuteron targets were part of the historic Stanford SLAC-MIT experiments of the late 1960s and early 1970s [87]. The natural place to continue studies of the nucleon and nuclear structure functions at high x and moderate Q^2 is Jefferson Lab (JLab) with its high intensity electron accelerator and large acceptance spectrometer facilities. The proposed energy upgrade [16] of the continuous electron beam accelerator of JLab will offer a unique opportunity to perform electron deep inelastic scattering studies off the $A=3$ system, as has been recently proposed [88,89]. The proposal calls for precise measurements of the ^{3}He and ^{3}H inelastic cross sections, under identical conditions, using an 11-GeV upgraded electron beam of JLab and the Hall A Facility of JLab. The inelastic electron-nucleus cross section is given in terms of the unpolarized structure functions F_1 and F_2 by

$$\sigma \equiv \frac{d^2\sigma}{d\Omega dE'}(E_o,E',\theta) = \frac{4\alpha^2(E')^2}{Q^4}\cos^2(\theta/2)\left[\frac{F_2^A(\nu,Q^2)}{\nu}+\frac{2F_1^A(\nu,Q^2)}{M_A}\tan^2(\theta/2)\right], \tag{49}$$

where α is the fine structure constant, E_o is the incident electron energy, E' and θ are the scattered electron energy and angle, $\nu=E_o-E'$ is the energy transfer, and M_A is the nuclear mass.

The structure functions F_1^A and F_2^A are connected through the ratio $R^A=\sigma_L^A/\sigma_T^A$ by

$$F_1^A=\frac{F_2^A(1+Q^2/\nu^2)}{2x(1+R^A)}, \tag{50}$$

where σ_L^A and σ_T^A are the nuclear virtual photoabsorption cross sections for longitudinally and transversely polarized photons. The ratio R^A has been measured to be independent of the mass number A in precise SLAC and CERN measurements using hydrogen, deuterium, iron, and other nuclei (for a compilation of data, see Ref. [1]).

By performing the tritium and helium measurements, under identical conditions using the same incident beam and scattered electron detection system configurations (same E_o, E' and θ), and assuming that the ratio R^A is the same for both nuclei, the ratio of the inelastic cross sections for the two nuclei provides a direct measurement of the ratio of the F_2 structure functions:

$$\frac{\sigma^{^3\mathrm{H}}(E_o,E',\theta)}{\sigma^{^3\mathrm{He}}(E_o,E',\theta)}=\frac{F_2^{^3\mathrm{H}}(\nu,Q^2)}{F_2^{^3\mathrm{He}}(\nu,Q^2)}. \tag{51}$$

The key issue for this experiment will be the availability of a high density tritium target planned for the Hall A Facility of JLab [90]. Tritium targets have been used in the past to measure the elastic form factors of ^{3}H at Saclay [91] and MIT-Bates [92]. The Saclay target contained liquid ^{3}H at 22 K and was able to tolerate beam currents up to 10 μA with very well understood beam-induced density changes. The nominal tritium density of 0.271 g/cm^3 at the operating conditions of this target was known, from actual density measurements, to $\pm 0.5\%$ accuracy. The MIT-Bates target contained ^{3}H gas at 45 K and 15 atm, and was able to tolerate beam currents up to 25 μA with small measurable beam-induced density changes. The tritium density, under these operating conditions, was determined to be 0.218 mg/cm^2 with $\pm 2\%$ uncertainty, using the virial formalism for hydrogen.

Given a high density tritium target, an entire program of elastic, quasielastic, and inelastic measurements will be possible at JLab. This program can be better accomplished by building a target similar to the one used at MIT-Bates (the cooling mechanism of a target similar to the Saclay one would prevent coincidence measurements). The tritium density can be better determined from comparison of the elastic cross section measured with the 45 K/15 atm cell and a cell filled up with tritium at higher temperatures (ideal gas of known density). Two more cells will also be necessary for the ^{3}He measurements.

The large solid angle and the wide kinematical coverage of the proposed medium acceptance device (MAD) Hall A spectrometer [93] will facilitate precise inelastic cross section measurements (statistical errors of $\leqslant \pm 0.25\%$) in a large x range as well as valuable systematics checks using reasonably short amounts of beam time. An important systematic check would be the confirmation that the ratio R is the same for ^{3}H and ^{3}He. The performance of the above spectrometer is expected to be comparable, if not better, to that of the SLAC 8 GeV/c spectrometer [27] that has provided precise measurements for absolute inelastic cross sections, inelastic cross section ratios, and differences in R for several nuclei [94–96]. The overall systematic errors for these measurements have been typically $\pm 2\%$, $\pm 0.5\%$, and $\pm 0.01\%$, respectively. Since the objective of the experiment is the measurement of cross section ratios rather than absolute cross sections, many of the experimental errors that

TABLE I. Kinematics of the proposed JLab experiment [88,89] on the measurement of the F_2^n/F_2^p ratio using ^{3}H and ^{3}He targets for an incident electron energy of 11 GeV (see text). The parameter W^2 is the invariant mass of the final hadronic state. The last column is the estimated ratio of the pion background to the scattered electron signal.

x	W^2 $(\mathrm{GeV/c})^2$	Q^2 $(\mathrm{GeV/c})^2$	E' (GeV)	θ (deg)	π/e
0.82	4.0	13.8	2.00	46.6	52
0.77	4.7	12.9	2.10	43.8	43
0.72	5.5	11.9	2.20	41.0	36
0.67	6.2	10.9	2.35	37.8	27
0.62	6.9	9.8	2.55	34.4	19
0.57	7.6	8.9	2.65	32.1	19
0.52	8.3	8.1	2.75	29.9	18
0.47	9.0	7.2	2.85	27.7	19
0.42	9.6	6.3	3.00	25.2	18
0.37	10.2	5.5	3.10	23.1	19
0.32	10.7	4.6	3.30	20.6	18
0.27	11.2	3.8	3.50	18.1	18
0.22	11.6	3.0	3.65	15.8	19

plague absolute measurements will cancel out. The experimental uncertainties on the ratio of cross sections should be similar to those achieved by SLAC experiments E139 [94] and E140 [95,96], which were typically around $\pm 0.5\%$.

Deep inelastic scattering with an upgraded 11-GeV JLab electron beam can provide measurements for the ^{3}H and ^{3}He F_2 structure functions in x ranging from 0.10 to 0.82. The electron scattering angle will range from 12° to 47° and the electron scattered energy from 1.0 to 6.0 GeV. It is assumed that the MAD spectrometer system will be instrumented with a threshold gas Cerenkov counter and a segmented lead-glass calorimeter, which will provide discrimination between scattered electrons and an associated hadronic (mostly pion) background. The above two-counter combination has provided in the past a pion rejection factor of at least 10 000 to 1 [95] that has allowed inelastic cross section measurements with negligible pion contamination for cases where the ratio of pion background to electron signal (π/e) was as large as 300. The expected π/e ratio for this experiment has been estimated using SLAC data from measurements of photon-nucleon cross sections [97] and is less than 300. The estimated π/e ratios are given in Table I along with the kinematical parameters for the proposed ''core'' set of measurements of the ratio $F_2^{^3\mathrm{H}}/F_2^{^3\mathrm{He}}$ up to $x=0.82$.

The estimated inelastic cross sections, counting rates, and the beam time required for the above measurements are given in Table II, assuming ^{3}H and ^{3}He luminosities of $\sim 5\times 10^{37}\ \mathrm{cm}^{-2}\,\mathrm{s}^{-1}$. The rates have been estimated under the assumption that $\sigma^{^3\mathrm{He}} \simeq \sigma_d + \sigma_p$ and $\sigma^{^3\mathrm{H}} \simeq 2\sigma_d - \sigma_p$, using values for the proton (σ_p) and deuteron (σ_d) inelastic cross sections and for the ratio R from the SLAC ''global'' analysis [3] of all available SLAC data. The rates are based on the MAD design specifications and include an approximation of radiative effects. It is evident from the listed rates that the proposed experiment will be able to provide very high statistics data and perform necessary systematic studies in a timely manner.

The 11-GeV beam and the momentum and angular range of MAD will allow measurements of R in the same x range as in the SLAC experiments by means of a Rosenbluth separation versus $\epsilon = [1 + 2(1+\nu^2/Q^2)\tan^2(\theta/2)]^{-1}$ (the degree of the longitudinal polarization of the virtual photon mediating the scattering). The R measurements will be limited by inherent systematics uncertainties rather than statistical uncertainties as in the SLAC case. It is estimated that the R measurements will require an amount of beam time comparable to the one required for the core set of measurements listed in Table II.

TABLE II. Estimated values of the ^{3}He and ^{3}H inelastic cross sections for the kinematics of Table I, expected scattered electron counting rates using JLab Hall A planned facilities (see text), and required amounts of beam time for $\pm 0.25\%$ cross section statistical uncertainties.

x	$\sigma^{^3\mathrm{He}}$ (nb/sr/GeV)	$\sigma^{^3\mathrm{H}}$ (nb/sr/GeV)	^{3}He rate (events/h)	^{3}H rate (events/h)	^{3}He time (h)	^{3}H time (h)
0.82	0.0146	0.0117	1.55×10^4	1.25×10^4	10.3	12.8
0.77	0.0308	0.0240	3.55×10^4	2.77×10^4	4.5	5.8
0.72	0.0639	0.0491	8.01×10^4	6.16×10^4	2.0	2.6
0.67	0.130	0.0996	1.80×10^5	1.38×10^5	0.9	1.2
0.62	0.261	0.202	4.02×10^5	3.12×10^5	0.5	0.5
0.57	0.463	0.364	7.76×10^5	6.10×10^5	0.5	0.5
0.52	0.801	0.639	1.43×10^6	1.14×10^6	0.5	0.5
0.47	1.35	1.10	2.51×10^6	2.04×10^6	0.5	0.5
0.42	2.35	1.95	4.58×10^6	3.80×10^6	0.5	0.5
0.37	3.89	3.30	7.84×10^6	6.65×10^6	0.5	0.5
0.32	7.00	6.07	1.50×10^7	1.30×10^7	0.5	0.5
0.27	12.8	11.3	2.91×10^7	2.58×10^7	0.5	0.5
0.22	23.3	21.1	5.53×10^7	5.01×10^7	0.5	0.5

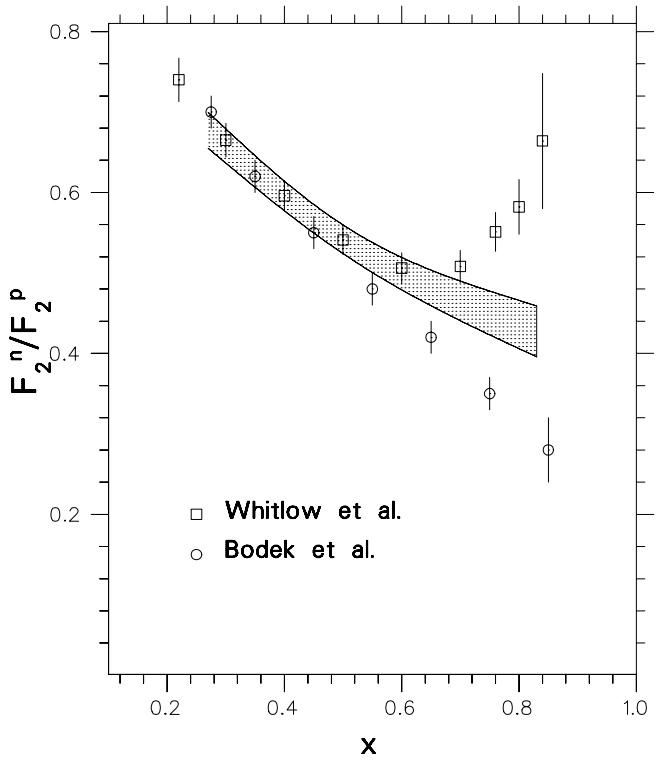

FIG. 12. Two diverging extractions [3,27] (see text and Fig. 1) of the ratio F_2^n/F_2^p from the same SLAC data on inelastic proton and deuteron scattering. The shaded band represents a $\pm$ one standard deviation error band for the proposed ^{3}H and ^{3}He JLab experiment [88,89]. The central values of the band are chosen arbitrarily to follow the trend of the analysis of the same data by Melnitchouk and Thomas [6].

The $F_2^{^3\mathrm{H}}/F_2^{^3\mathrm{He}}$ ratio is expected to be dominated by experimental uncertainties that do not cancel in the inelastic cross section ratio of ^{3}H to ^{3}He and by the theoretical uncertainty in the calculation of the ratio $\mathcal{R}$. Assuming that the target densities can be known to the $\pm 0.5\%$ level and that the relative difference in the ^{3}H and ^{3}He radiative corrections would be $\pm 0.5\%$ as in Refs. [94,95], the total experimental error in the the inelastic cross section ratio of ^{3}H to ^{3}He should be $\sim \pm 1.0\%$. Such an error is comparable to a realistic maximum theoretical uncertainty ($\sim \pm 1\%$ in the vicinity of $x=0.8$) in the calculation of the ratio $\mathcal{R}$.

The quality of the expected F_2^n/F_2^p extracted values is shown in Fig. 12. The two sets of data in this figure represent the extreme possible values for the ratio F_2^n/F_2^p (see Fig. 1) and are indicative of the present uncertainties in the nuclear corrections in the extraction of F_2^n/F_2^p from proton and deuterium inelastic scattering data. The shaded band represents the projected uncertainty ($\pm$ one standard deviation error band) of the proposed JLab measurement. The band assumes a $\pm 1\%$ overall systematic experimental error in the measurement of the $\sigma^{^3\mathrm{H}}/\sigma^{^3\mathrm{He}}$ ratio and a theoretical uncertainty in $\mathcal{R}$ that increases linearly from 0% at $x=0$ to $\pm 1\%$ at $x=0.82$. The central value of the projected JLab band has been arbitrarily chosen, for this comparison purpose, to follow the trend obtained in the relativistic analysis of nuclear binding and Fermi motion of Ref. [6] (see Fig. 1). It is evident that the proposed measurement will be able to unquestionably distinguish between the present competing extractions of the F_2^n/F_2^p ratio from proton and deuterium inelastic measurements, and determine its value with an unprecedented precision in an almost model-independent way.

A secondary goal of this proposed experiment would be the precise determination of the EMC effect in ^{3}H and ^{3}He. At the present time, the available SLAC and CERN data allow for two equally compatible parametrizations [94] of the EMC effect, within the achieved experimental uncertainties. In the first parametrization, the EMC effect is parametrized versus the mass number A, and in the second one versus the nuclear density ρ. While the two parametrizations are indistinguishable for heavy nuclei, they predict quite distinct patterns for $A=3$. The expected precision ($\pm 1\%$) of this experiment for the $F_2^{^3\mathrm{H}}/F_2^{^3\mathrm{He}}$ ratio should easily allow to distinguish between the two competing parametrizations.

VI. CONCLUSIONS

We have presented a comprehensive analysis of deep inelastic scattering from ^{3}He and ^{3}H nuclei, focusing in particular on the extraction of the free neutron structure function at large x. We have demonstrated the effectiveness of using the mirror symmetry of $A=3$ nuclei to extract the ratio of the neutron to proton structure functions, F_2^n/F_2^p, free of nuclear effects to $\lesssim 1-2\,\%$ for all $x \lesssim 0.8$. This is comparable with the expected experimental errors for the simultaneous measurement of ^{3}He and ^{3}H DIS cross sections at an energy-upgraded Jefferson Lab, for instance.

The major theoretical uncertainty involved in the extraction is that associated with the nuclear wave functions of ^{3}He and ^{3}H. We have examined two independent methods of calculating the nuclear spectral function, namely, by solving the Faddeev equations, and using a variational approach, for a range of two-body interactions. The resulting structure function ratios have been studied as a function of x and Q^2 for various input nucleon structure function parametrizations. By utilizing an iterative procedure, the dependence of the extracted F_2^n on input parametrizations can be effectively removed altogether. We find that this procedure converges quite rapidly, requiring only ~ 3 iterations.

We have also considered explicit charge-symmetry breaking effects in the nuclear wave functions, effects associated with the medium modification of the bound nucleon structure functions, as well as corrections to the impulse approximation arising from non-nucleonic degrees of freedom such as six-quark clusters. In all cases consistent with existing nuclear phenomenology we find that the nuclear effects in the ratio $\mathcal{R}$ of ^{3}He to ^{3}H EMC ratios cancel to within $1-2\,\%$ at the relevant kinematics, making this an extremely robust method with which to extract the free-neutron structure function, and thus settle a ''textbook'' issue which has eluded a definitive resolution for nearly three decades.

Once the F_2^n/F_2^p ratio is determined, one can combine the free-proton and deuteron data to obtain the size of the EMC

effect in the deuteron, which remains a source of controversy, via

$$R(d) = \frac{F_2^d}{F_2^p(1 + F_2^n/F_2^p|_{\rm extr})}, \tag{52}$$

where $F_2^n/F_2^p|_{\rm extr}$ is the neutron to proton ratio extracted from Eq. (5).

While the ratio $\mathcal{R}$ is not very sensitive to nuclear dynamics in the $A=3$ system, measurement of the absolute ^{3}He to ^{3}H cross sections will, on the other hand, enable one to discriminate between different models. In particular, it will allow the completion of the empirical study of nuclear effects in deep inelastic scattering over the full range of mass numbers.

ACKNOWLEDGMENTS

This work was supported by the Australian Research Council, the U.S. Department of Energy Contract No. DE-AC05-84ER40150, under which the Southeastern Universities Research Association (SURA) operates the Thomas Jefferson National Accelerator Facility (Jefferson Lab), the U.S. Department of Energy Contract No. DE-FG02-01ER41200, and the U.S. National Science Foundation Grant No. PHY-0072384.

[1] D.F. Geesaman, K. Saito, and A.W. Thomas, Annu. Rev. Nucl. Part. Sci. **45**, 337 (1995).
[2] J.J. Aubert *et al.*, Phys. Lett. **123B**, 275 (1983).
[3] L.W. Whitlow *et al.*, Phys. Lett. B **282**, 475 (1992).
[4] L.L. Frankfurt and M.I. Strikman, Phys. Rep. **160**, 235 (1988).
[5] S. Liuti and F. Gross, Phys. Lett. B **356**, 157 (1995).
[6] W. Melnitchouk and A.W. Thomas, Phys. Lett. B **377**, 11 (1996).
[7] W. Melnitchouk, J. Speth, and A.W. Thomas, Phys. Lett. B **435**, 420 (1998).
[8] P. Souder, *Proceedings of the Workshop on CEBAF at Higher Energies CEBAF* (CEBAF, Newport News, 1994); R. Michaels, *Physics and Instrumentation with 6–12 GeV Beams* (Jefferson Lab, Newport News, 1998), p. 347.
[9] W. Melnitchouk and J.C. Peng, Phys. Lett. B **400**, 220 (1997).
[10] C. Adloff *et al.*, Eur. Phys. J. C **13**, 609 (2000); J. Breitweg *et al.*, *ibid.* **12**, 411 (2000).
[11] H. Fenker, C. Keppel, S. Kuhn, and W. Melnitchouk (spokespersons), Jefferson Lab experiment E03-012.
[12] L.L. Frankfurt and M.I. Strikman, Phys. Rep. **76**, 215 (1981); S. Simula, Phys. Lett. B **387**, 245 (1996); W. Melnitchouk, M. Sargsian, and M.I. Strikman, Z. Phys. A **359**, 99 (1997).
[13] G. G. Petratos *et al.*, *Proceedings of the Workshop on Experiments with Tritium at JLab* (Jefferson Lab, Newport News, 1999).
[14] I.R. Afnan, F. Bissey, J. Gomez, A.T. Katramatou, W. Melnitchouk, G.G. Petratos, and A.W. Thomas, Phys. Lett. B **493**, 36 (2000).
[15] W. Melnitchouk and A.W. Thomas, nucl-th/0207056.
[16] *The Science Driving the 12 GeV Upgrade*, edited by L. Cardman *et al.* (Jefferson Lab, Newport News, 2001).
[17] K. Ackerstaff *et al.*, Phys. Lett. B **475**, 386 (2000).
[18] R. P. Feynman, *Photon Hadron Interactions* (Benjamin, Reading, MA, 1972).
[19] F.E. Close, Phys. Lett. **43B**, 422 (1973).
[20] F.E. Close and A.W. Thomas, Phys. Lett. B **212**, 227 (1988).
[21] R. Carlitz, Phys. Lett. **58B**, 345 (1975).
[22] N. Isgur, Phys. Rev. D **59**, 034013 (1999).
[23] G.R. Farrar and D.R. Jackson, Phys. Rev. Lett. **35**, 1416 (1975).
[24] W. Melnitchouk, Phys. Rev. Lett. **86**, 35 (2001).
[25] F. E. Close and W. Melnitchouk, hep-ph/030213 (to be published).
[26] A. Bodek and J.L. Ritchie, Phys. Rev. D **23**, 1070 (1981); **24**, 1400 (1981).
[27] A. Bodek *et al.*, Phys. Rev. D **20**, 1471 (1979).
[28] S. Platchkov *et al.*, Nucl. Phys. **A510**, 740 (1990).
[29] C. Adloff *et al.*, Z. Phys. C **74**, 191 (1997); J. Breitweg, *et al.*, *ibid.* **74**, 207 (1997).
[30] S. Kuhlmann, H.L. Lai, and W.K. Tung, Phys. Lett. B **409**, 271 (1997).
[31] W. Melnitchouk and A.W. Thomas, Phys. Lett. B **414**, 134 (1997); F.M. Steffens, W. Melnitchouk, and A.W. Thomas, Eur. Phys. J. C **11**, 673 (1999).
[32] S. Kuhlmann *et al.*, Phys. Lett. B **476**, 291 (2000).
[33] W. Melnitchouk, A.W. Schreiber, and A.W. Thomas, Phys. Rev. D **49**, 1183 (1994).
[34] T. Uchiyama and K. Saito, Phys. Rev. C **38**, 2245 (1988).
[35] F. Gross and S. Liuti, Phys. Rev. C **45**, 1374 (1992).
[36] S.A. Kulagin, W. Melnitchouk, G. Piller, and W. Weise, Phys. Rev. C **52**, 932 (1995).
[37] F. Bissey, V. Guzey, M.I. Strikman, and A.W. Thomas, Phys. Rev. C **65**, 64317 (2002).
[38] W. Melnitchouk, G. Piller, and A.W. Thomas, Phys. Lett. B **346**, 165 (1995); Phys. Rev. C **54**, 894 (1996).
[39] W. Melnitchouk, A.W. Schreiber, and A.W. Thomas, Phys. Lett. B **335**, 11 (1994).
[40] R. L. Jaffe, in *Relativistic Dynamics and Quark-Nuclear Physics*, edited by M. B. Johnson and A. Pickleseimer (Wiley, New York, 1985); H. Jung and G.A. Miller, Phys. Lett. B **200**, 351 (1988); U. Oelfke and P.U. Sauer, Nucl. Phys. **A518**, 593 (1990); P.J. Mulders, A.W. Schreiber, and H. Meyer, *ibid.* **A549**, 498 (1992).
[41] G. Piller and W. Weise, Phys. Rep. **330**, 1 (2000).
[42] L.P. Kaptari, A.I. Titov, E.L. Bratkovskaya, and A.Yu. Umnikov, Nucl. Phys. **A512**, 684 (1990).
[43] W. Melnitchouk and A.W. Thomas, Phys. Rev. D **47**, 3783 (1993); Phys. Lett. B **317**, 437 (1993).
[44] G.B. West, Phys. Lett. **37B**, 509 (1971); W.B. Atwood and G.B. West, Phys. Rev. D **7**, 773 (1973).
[45] C. Ciofi degli Atti and S. Liuti, Phys. Rev. C **41**, 1100 (1990); **44**, R1269 (1991).

[46] S.A. Kulagin, G. Piller, and W. Weise, Phys. Rev. C **50**, 1154 (1994).
[47] F. Bissey, A.W. Thomas, and I.R. Afnan, Phys. Rev. C **64**, 024004 (2001).
[48] C. Ciofi degli Atti, E. Pace, and G. Salme, Phys. Rev. C **21**, 805 (1980).
[49] C. Ciofi degli Atti, E. Pace, and G. Salme, Phys. Lett. **141B**, 14 (1984).
[50] L. D. Faddeev, *Mathematical Aspects of the Three-Body Problem* (Daniel Davey, New York, 1965).
[51] G.L. Payne, J.L. Friar, B.F. Gibson, and I.R. Afnan, Phys. Rev. C **22**, 823 (1980).
[52] E. W. Schmid and H. Ziegelmann, *The Quantum Mechanical Three-Body Problem* (Pergamon Press, New York, 1974).
[53] I.R. Afnan and N.D. Birrell, Phys. Rev. C **16**, 823 (1977).
[54] J. S. Levinger, *The Two and Three Body Problem*, Springer Tract in Modern Physics Vol. 71 (Springer-Verlag, Berlin, 1974).
[55] More accurately, φ_α is defined by the equation $|\varphi_\alpha\rangle = G_0 V_\alpha |\Psi\rangle$, where V_α is the potential between particles β and γ and $G_0 = (E - H_0)^{-1}$.
[56] W.C. Parke, Y. Koike, D.R. Lehman, and L.C. Maximon, Few-Body Syst. **11**, 89 (1991).
[57] I.R. Afnan and A.W. Thomas, Phys. Rev. C **10**, 109 (1974).
[58] I. R. Afnan and A. W. Thomas, in *Fundamentals of Three-Body Scattering Theory*, edited by A. W. Thomas, Modern Three-Hadron Physics Vol. 2 (Springer-Verlag, Berlin, 1977).
[59] J. Haidenbauer and W. Plessas, Phys. Rev. C **30**, 1822 (1984).
[60] T.Y. Saito and I.R. Afnan, Few-Body Syst. **18**, 101 (1995).
[61] R.V. Reid, Ann. Phys. (N.Y.) **50**, 411 (1968).
[62] Y. Yamaguchi and Y. Yamaguchi, Phys. Rev. **95**, 1635 (1954).
[63] The notation adopted in Sec. III B 2 differs slightly from that used in the Faddeev approach in Sec. III B 1, but is consistent with that used in the literature for variational calculations.
[64] P. Nunberg, D. Prosperi, and E. Pace, Nucl. Phys. **A285**, 58 (1977).
[65] C. Ciofi degli Atti, S. Simula, L.L. Frankfurt, and M.I. Strikman, Phys. Rev. C **44**, R7 (1991); C. Ciofi degli Atti and S. Simula, *ibid.* **53**, 1689 (1996).
[66] G.B. West, Phys. Rep. **18**, 263 (1975).
[67] H.L. Lai *et al.*, Eur. Phys. J. C **12**, 375 (2000).
[68] We also omit possible three-body forces since these are expected to have a negligible effect on $\mathcal{R}$.
[69] C. Ciofi degli Atti, D.B. Day, and S. Liuti, Phys. Rev. C **46**, 1045 (1992).
[70] A. Donnachie and P.V. Landshoff, Z. Phys. C **61**, 139 (1994).
[71] P. Amaudruz *et al.*, Nucl. Phys. **B371**, 3 (1992); M. Virchaux and A. Milsztajn, Phys. Lett. B **274**, 221 (1992).
[72] S. I. Alekhin, S. A. Kulagin, and S. Liuti. hep-ph/0304210.
[73] M. Gluck, E. Reya, and A. Vogt, Eur. Phys. J. C **5**, 461 (1998).
[74] S.J. Brodsky, M. Burkardt, and I. Schmidt, Nucl. Phys. **B441**, 197 (1995).
[75] E. Pace, G. Salme, and S. Scopetta, Nucl. Phys. **A689**, 453 (2001); E. Pace, G. Salme, S. Scopetta, and A. Kievsky, Phys. Rev. C **64**, 055203 (2001).
[76] A.Yu. Umnikov, F.C. Khanna, and L.P. Kaptari, Z. Phys. A **348**, 211 (1994); A. Höcker and V. Kartvelishvili, Nucl. Instrum. Methods Phys. Res. A **372**, 469 (1996).
[77] M.M. Sargsian, S. Simula, and M.I. Strikman, Phys. Rev. C **66**, 024001 (2002).
[78] S.A. Kulagin, Nucl. Phys. **A640**, 435 (1998).
[79] L.L. Frankfurt and M.I. Strikman, Nucl. Phys. **B250**, 1585 (1985).
[80] S. Dieterich *et al.*, Phys. Lett. B **500**, 47 (2001); R. Ransome, Nucl. Phys. **A699**, 360 (2002); S. Strauch *et al.*, nucl-ex/0211022 (to be published).
[81] W. Melnitchouk, K. Tsushima, and A.W. Thomas, Eur. Phys. J. A **4**, 105 (2002).
[82] W. Melnitchouk, F. Bissey, I.R. Afnan, and A.W. Thomas, Phys. Rev. Lett. **84**, 5455 (2000).
[83] C.W. de Jager, H. de Vries, and C. de Vries, At. Data Nucl. Data Tables **14**, 479 (1974).
[84] P. Hoodbhoy and R.L. Jaffe, Phys. Rev. D **35**, 113 (1987).
[85] M. Betz, G. Krein, and T.A.J. Maris, Nucl. Phys. **A437**, 509 (1985).
[86] P.J. Mulders and A.W. Thomas, Phys. Rev. Lett. **52**, 1199 (1984); M. Sato, S. Coon, H. Pirner, and J. Vary, Phys. Rev. C **33**, 1062 (1986); K.E. Lassila and U.P. Sukhatme, Phys. Lett. B **209**, 343 (1988).
[87] J.I. Friedman, H.W. Kendall, and R.E. Taylor, Rev. Mod. Phys. **63**, 573 (1991).
[88] G. G. Petratos *et al.*, *Proceedings of the International Workshop on Nucleon Structure in High x-Bjorken Region (HiX2000)* (Temple University, Philadelphia, 2000), nucl-ex/0010011.
[89] G. G. Petratos *et al.*, Report No. JLab PAC18 2000.
[90] R. D. Ransome, *Proceedings of the International Workshop on Nucleon Structure in High x-Bjorken Region (HiX2000)* (Temple University, Philadelphia, 2000).
[91] A. Amroun *et al.*, Nucl. Phys. **A579**, 596 (1994).
[92] D. Beck *et al.*, Nucl. Instrum. Methods Phys. Res. A **277**, 323 (1989).
[93] J. J. LeRose and P. Brinza, *Proceedings of International Workshop on the Nucleon Structure in the High-x Region*(Temple University, Philadelphia, 2000).
[94] J. Gomez *et al.*, Phys. Rev. D **49**, 4348 (1994).
[95] S. Dasu *et al.*, Phys. Rev. D **49**, 5641 (1994).
[96] L.H. Tao *et al.*, Z. Phys. C **70**, 387 (1996).
[97] D. E. Wiser, Ph.D. thesis, University of Wisconsin, 1977.